Photothermal Heterodyne Imaging of Individual Nonfluorescent Nanoclusters and Nanocrystals

Stéphane Berciaud, Laurent Cognet, Gerhard A. Blab, and Brahim Lounis

Centre de Physique Moléculaire Optique et Hertzienne, CNRS (UMR 5798) et Université Bordeaux I, 351, cours de la Libération, 33405 Talence Cedex, France

(Received 25 March 2004; published 13 December 2004)

We introduce a new, highly sensitive, and simple heterodyne optical method for imaging individual nonfluorescent nanoclusters and nanocrystals. A 2 order of magnitude improvement of the signal is achieved compared to previous methods. This allows for the unprecedented detection of individual small absorptive objects such as metallic clusters (of 67 atoms) or nonluminescent semiconductor nanocrystals. The measured signals are in agreement with a calculation based on the scattering field theory from a photothermal-induced modulated index of refraction profile around the nanoparticle.

DOI: 10.1103/PhysRevLett.93.257402 PACS numbers: 78.67.–n

In the fast evolving field of nanoscience, where size is crucial for the properties of the objects, simple and sensitive methods for the detection and characterization of single nanoclusters and nanocrystals (nano-objects) are needed. The most commonly used optical techniques are based on luminescence. Single fluorescent molecules have been studied on their own and are now routinely applied in various research domains ranging from quantum optics [1–3] to life science [4]. Yet, fluorescent molecules allow only for short observation times due to inherent photobleaching. The development of brighter and more stable luminescent objects, such as semiconductor nanocrystals [5,6], has remedied some of this shortcoming, but this improvement has come at the price of a strong blinking behavior.

An interesting alternative to fluorescence methods relies solely on the absorptive properties of the object. At liquid helium temperatures single molecules were initially detected by an absorption technique owing to the high quality factor of the zero-phonon line which gives a considerable absorption cross section at resonance [7] (few 10^{-11} cm^2). Single ions or atoms isolated in rf traps [8] or high Q cavities [9,10] have been detected by absorption of a probe beam. In general, particles with large absorption cross sections and short time intervals between successive absorption events are likely candidates for detection with absorption methods [8].

Metal nanoparticles fulfill both of these requirements: excited near their plasmon resonance a nanometer sized gold nanoparticle has a relatively large absorption cross section ($\sim 8 \times 10^{-14}$ cm^2 for a 5 nm diameter particle) and a fast electron-phonon relaxation time (in the picosecond range [11]). Since luminescence from these particles is extremely weak, almost all the absorbed energy is converted into heat. The temperature rise induced by the heating leads to a variation of the local index of refraction. Previously, a polarization interference contrast technique has been developed [12] to detect this photothermal effect. In that case, the signal is caused by the phase shift induced between the two spatially separated beams of an interferometer, where only one of the beams propagates through the heated region, and images of 5 nm diameter gold nanoparticles have been recorded with a signal-to-noise (SNR) ratio $\sim$10. Also, the sensitivity of this technique, although high, is ultimately limited by the quality of the overlap of the two arms of the interferometer as well as by their relative phase fluctuations.

In this Letter we introduce a new, more sensitive, and much simpler method for detecting nonfluorescent nano-objects. It uses a single probe beam which produces a frequency-shifted scattered field as it interacts with time-modulated variations of the refraction index around an absorbing nano-object. The scattered field is detected by its beatnote with the probe field which plays the role of a local oscillator as in the heterodyne technique. Because this new method is not subject to the limitations mentioned above, a 2 order of magnitude improvement of the sensitivity is achieved compared to the previous photothermal method. This allows for the unprecedented detection of small absorptive objects such as individual metallic clusters composed of 67 atoms.

When a small gold nanoparticle (or any absorbing nano-object) embedded in a homogeneous medium is illuminated with an intensity modulated laser beam, it behaves like a heat point source with a heating power $P_{\text{heat}}[1 + \cos(\Omega t)]$, Ω being the modulation frequency and P_{heat} the average absorbed laser power. It generates a time-modulated index of refraction in the vicinity of the particle with a spatiotemporal profile given by [13] $\Delta n(r, t) = \frac{\partial n}{\partial T} \frac{P_{\text{heat}}}{4\pi\kappa r}[1 + \cos(\Omega t - \frac{r}{R_{\text{th}}})e^{-r/R_{\text{th}}}]$, with r the distance from the particle, n the index of refraction of the medium, $\frac{\partial n}{\partial T}$ its variations with temperature ($\sim 10^{-4}$ K^{-1}), $R_{\text{th}} = \sqrt{2\kappa/\Omega C}$ the characteristic length for heat diffusion, κ the thermal conductivity of the medium, and C its heat capacity per unit volume. A probe beam interacting with this profile gives rise to a scattered

field containing sidebands with frequency shifts Ω. As any heterodyne technique, interference between a reference field E_{ref} [either the reflection of the incident probe at the interface between a coverslip and the sample or its transmission; see Fig. 1(a)] and the scattered field produces a beatnote at the modulation frequency Ω which can be easily extracted with a lock-in amplifier.

In practice, we overlay a (red) probe beam (720 nm, single frequency Ti:sapphire laser) and a (green) heating beam (532 nm, frequency doubled Nd:YAG laser) whose intensity is modulated at Ω (100 kHz to 15 MHz) by an acousto-optic modulator [see Fig. 1(a)]. Using a high aperture objective (100 $\times$, Zeiss, NA = 1.4), both beams are focused onto the same spot on the sample. A combination of a polarizing cube and a quarter wave plate is used to extract the interfering reflected field (so-called reference field) and backward scattered field. Optionally, a second microscope objective can be employed to efficiently collect the interfering probe-transmitted and forward-scattered fields. The power of the heating beam ranged from less than 1 μW to 3.5 mW (depending on the nanoparticle size to be imaged) at the objective. Reflected or transmitted red beams are collected on fast photodiodes and fed into a lock-in amplifier to detect the beat signal at Ω. Throughout the experiment, we used an integration time of 10 ms. A microscopy image was formed by moving the sample over the fixed laser spots by means of a 2D piezoscanner.

The samples were prepared by spin coating a solution of gold nanoparticles [diameter of 1.4, 2, 5, 10, 20, 33, or 75 nm, diluted into a polyvinyl-alcohol (PVOH) matrix, 2% mass] onto clean microscope coverslips. The dilution and spinning speed were chosen such that the final density of spheres in the sample was less than 1 $\mu\mathrm{m}^{-2}$. Application of a silicon oil on the sample ensures homogeneity of the heat diffusion. The size distribution of the nanospheres was checked by transmission electron microscopy (data not shown) and was in agreement with the manufacturer's specification.

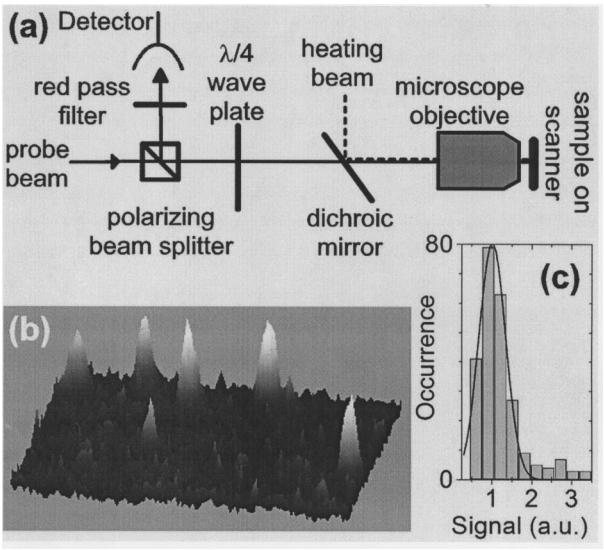

FIG. 1. (a) Schematic of the experiment. (b) 3D representation of a photothermal heterodyne image (5×5 $\mu\mathrm{m}^2$) containing individual 67 atom gold clusters (1.4 nm diameter). (c) Signal histogram of 272 peaks detected in a sample prepared with 67 atom gold clusters. The monomodal shape of the distribution reveals that individual clusters are detected.

Figure 1(b) shows a three-dimensional representation of a photothermal heterodyne image of small gold aggregates of 67 atoms (1.4 nm nanogold). The image shows no background from the substrate, which means that the signal arises from the only absorbing objects in the sample, namely, the gold aggregates. They are detected with a relatively small heating power ($\sim$3.5 mW) and a remarkably large signal-to-noise ratio (SNR $>$ 10). We further confirmed that the peaks stem from single particles by generating the histogram of the signal height for 272 imaged peaks [Fig. 1(c)]. We found a monomodal distribution with a width in agreement with the spread in particle size.

In order to estimate the measured signal, we have used the theory of "scattering from a fluctuating dielectric medium" [14] to calculate the field scattered by the modulated index profile $\Delta n(r, t)$. The beating at Ω between the reference and scattered fields leads to a beating power S at the detector with two terms in quadrature [15]:

$$S = \alpha n \frac{\partial n}{\partial T} \sqrt{I_{\mathrm{inc}}} \sqrt{P_{\mathrm{ref}}} \frac{P_{\mathrm{heat}}}{C\lambda^2} \frac{1}{\Omega} [f_\kappa(\Omega) \cos(\Omega t) + g_\kappa(\Omega) \sin(\Omega t)], \quad (1)$$

with α a geometry factor close to unity, I_{inc} the incident red intensity at the particle location, and P_{ref} the reference (backreflected) beam power. $f_\kappa(\Omega)$ and $g_\kappa(\Omega)$ are two dimensionless functions which depend on the modulation frequency and the thermal diffusivity of the medium. The variations of $f_\kappa(\Omega)/\Omega$ and $g_\kappa(\Omega)/\Omega$ are presented in Fig. 2(a) for $\kappa/C = 2 \times 10^{-8}$ m^2/s. At low frequencies, the characteristic length of the heat diffusion R_{th} is larger than the probe spot size ($\sim \lambda/2$) and the term $f_\kappa(\Omega)/\Omega$, in phase with the applied modulation, is preponderant. However, at sufficiently high frequencies such that $R_{\mathrm{th}} \ll \lambda$, the quadrature term $g_\kappa(\Omega)/\Omega$ dominates and decreases as $1/\Omega$.

The magnitude of demodulated signal delivered by the lock-in amplifier is proportional to

$$S_{\mathrm{dem}} \propto \sqrt{\langle S(t)^2 \rangle_t} \propto \frac{1}{\Omega} \sqrt{f_\kappa(\Omega)^2 + g_\kappa(\Omega)^2}. \quad (2)$$

The frequency dependence of this signal measured on single particles is presented in Fig. 2. A good quantitative agreement with the theoretical form of S_{dem} is obtained.

To further ensure the validity of our calculations, we used Eq. (1) to estimate the beating power at the detector. A single 2 nm gold nanoparticle has an absorption cross

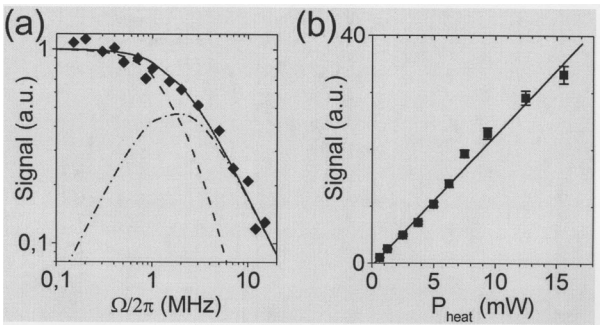

FIG. 2. (a) Measured dependence of the signal (diamonds) on the modulation frequency Ω measured on a single 5 nm nanoparticle and comparison with theory using Eq. (2) (solid line). The variations of $f_\kappa(\Omega)/\Omega$ (dashed line) and $g_\kappa(\Omega)/\Omega$ (dash-dotted line) are also presented. (b) Signal obtained from an individual 5 nm gold nanoparticle (squares) as a function of the incident power. The data are adjusted by a linear fit (solid line).

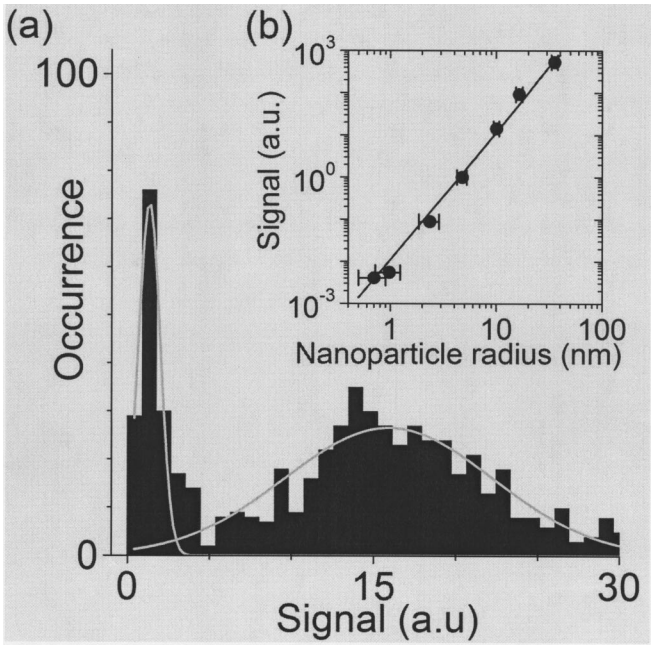

FIG. 3. (a) Signal distribution obtained from a sample containing both 2 and 5 nm gold nanoparticles. (b) Size dependence of the signal, i.e., absorption cross section (circles) deduced from a series of histograms as presented in (a) and in comparison to the Mie theory (solid line).

section of $\sim 5 \times 10^{-15}$ cm^2 at 532 nm and will absorb $P_{\text{heat}} = 10$ nW when illuminated by a laser intensity of 2 MW/cm^2. For a probe incident power $P_{\text{inc}} = 70$ mW, a frequency $\Omega/2\pi = 800$ kHz, and a reference power $P_{\text{ref}} = 100$ μW, Eq. (2) gives the beating power $S_{\text{dem}} \sim 5$ nW. After calibration of the detection chain, we measured a beating power of ~ 2 nW in qualitative agreement with the theoretical prediction. Figure 2(b) shows a linear dependence of the signal with heating power. A further increase on the power is not accompanied by saturation but leads to fluctuations in the signal amplitude and eventually irreversible damage on the particle [16,17].

As a first application of this method, we studied the size dependence of the absorption cross section of gold nanoparticles (at 532 nm, close to the maximum of the plasmon resonance) with diameters ranging from 1.4 to 75 nm. To do so, we prepared different samples containing nanoparticles of two different (successive) sizes (1.4 and 5 nm, 2 and 5 nm, 5 and 10 nm, up to 33 and 75 nm). For each sample, a histogram of the signal amplitudes was generated, as exemplified in Fig. 3. All the histograms displayed bimodal distributions and the mean of each population was measured. This allows us to report the size dependence of the absorption cross section normalized to that of 10 nm particles [Fig. 3(b)]. As expected by the Mie scattering theory, we find a good qualitative agreement with a third-order law of the absorption cross section versus the radius of the particles [17] [solid line in Fig. 3(b)]. By removing ensemble averaging, this approach opens up the possibility to investigate the size dependent optical material functions of small metal clusters such as the dielectric permittivity [18].

As shown in Fig. 1, we are now able to detect metal nanoparticles as small as 1.4 nm in diameter with a good SNR (>10) which is shot-noise limited. To our knowledge, this is the first time that such small aggregates are being detected with purely optical methods. While the absorption cross section of these clusters is only of the order of 10^{-15} cm^2, comparable to that of a good fluorophore, or CdSe/ZnS nanocrystals [19,20], their relaxation times are very short. In contrast, luminescent semiconductor nanocrystals or fluorescent molecules have radiative relaxation times in the nanosecond range, which renders them difficult to be detected by their absorption. However, at relatively high excitation intensities, semiconductor nanocrystals do no longer exhibit luminescence. Efficient nonradiative relaxation pathways open up with short relaxation times relying on Auger multiexciton relaxation processes [21,22], which make them detectable by our method. Figure 4(a) shows a fluorescent image of luminescent colloidal CdSe/ZnS quantum dots (peak emission at 640 nm) excited by the heating beam at very low intensities (0.1 kW/cm^2). The blinking behavior characteristic of single quantum dot emission is clearly visible in the image [23]. A photothermal heterodyne image of the same region was recorded afterwards at an excitation intensity of 5 kW/cm^2 where quantum dots are no longer luminescent [Fig. 4(b)]. The two images correlate well, ensuring that the spots in the photothermal heterodyne image are indeed individual quantum dots ($>90\%$ of the fluorescent spots correlate with a photothermal spot). They do not show any blinking behavior. Interestingly, initially nonfluorescent quantum dots [absent from Fig. 4(a)] are now detected by the photothermal technique.

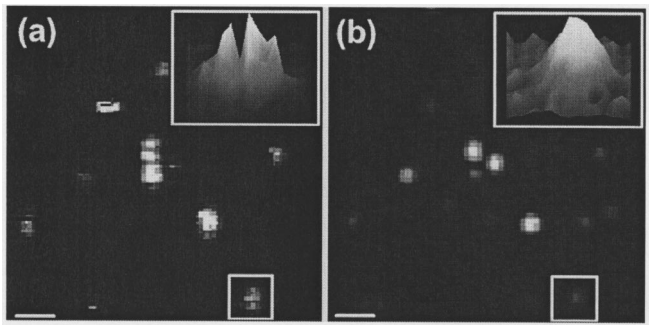

FIG. 4. Comparison of luminescence (a) and photothermal (b) images of the same area in a sample containing CdSe/ZnSe semiconductor nanocrystals. The insets show a zoom of one individual quantum dot marked by a square in the lower right of each image. The scale bar is 1 μm.

For biological applications, the temperature rise at the surface of the nanoparticle is an important issue [24]. In the current configuration, a 5 nm gold nanoparticle can be detected with a SNR > 100 at a heating power of 1 mW. At this power, we estimate a local temperature increase of 4 K in aqueous solutions. As the temperature reduces as the inverse of distance, and most conceivable microscopy applications in biosciences do not require such a high SNR, the method presented in this Letter will permit one to image small gold particles by inducing a local heating of far less than 1 K above the average temperature in the sample.

The present work demonstrates the advantages of photothermal heterodyne detection for absorbing nanoobjects. As any far-field optical technique, it has a wavelength limited resolution. An interesting challenge would now be to combine the unprecedented sensitivity of the method presented here with the subwavelength resolution of near-field optical techniques [25]. The study of the physical properties of very small metallic aggregates or nonluminescent semiconductor nanocrystals is now possible at the individual object level. This photothermal method does not suffer from the drawbacks of blinking and photobleaching and is immune to the effects of fluorescing and scattering backgrounds. It could be applied to many diffusion and colocalization problems in physical chemistry and material science and to track labeled biomolecules in cells.

We wish to thank A. Brisson and O. Lambert for their assistance with electron microscopy experiments, P. Tamarat and O. Labeau for their help with the quantum dots, and M. Orrit and D. Choquet for helpful discussions. G. A. B. acknowledges financial support from FWF (Schrödinger-Stipendium) and the Fondation pour la Recherche Médicale. This research was funded by CNRS (ACI Nanoscience and DRAB), by Région Aquitaine, and by the French Ministry for Education and Research (MENRT).

[1] P. Tamarat *et al.*, J. Phys. Chem. A **104**, 1 (2000).
[2] B. Lounis and W. E. Moerner, Nature (London) **407**, 491 (2000).
[3] C. Hettich *et al.*, Science **298**, 385 (2002).
[4] Special Issue, Science **283** (1999).
[5] A. P. Alivisatos, Science **271**, 933 (1996).
[6] B. O. Dabbousi *et al.*, Appl. Phys. Lett. **66**, 1316 (1995).
[7] W. E. Moerner and L. Kador, Phys. Rev. Lett. **62**, 2535 (1989).
[8] D. J. Wineland, W. M. Itano, and J. C. Bergquist, Opt. Lett. **12**, 389 (1987).
[9] C. J. Hood *et al.*, Science **287**, 1447 (2000).
[10] P. Pinske *et al.*, Nature (London) **404**, 365 (2000).
[11] A. Arbouet *et al.*, Phys. Rev. Lett. **90**, 177401 (2003).
[12] D. Boyer *et al.*, Science **297**, 1160 (2002).
[13] H. S. Carslaw and J. C. Jaeger, *Conduction of Heat in Solids* (Oxford University Press, Oxford, 1993).
[14] B. Chu, *Laser Light Scattering* (Academic Press, New York, 1974).
[15] S. Berciaud *et al.* (to be published).
[16] A. Takami, H. Kurita, and S. Koda, J. Phys. Chem. B **103**, 1226 (1999).
[17] S. Link and M. A. El-Sayed, J. Phys. Chem. B **103**, 8410 (1999).
[18] U. Kreibig and M. Vollmer, *Optical Properties of Metal Clusters* (Springer-Verlag, Berlin, 1995).
[19] B. Lounis *et al.*, Chem. Phys. Lett. **329**, 399 (2000).
[20] C. Leatherdale *et al.*, J. Phys. Chem. B **106**, 7619 (2002).
[21] L. Wang *et al.*, Phys. Rev. Lett. **91**, 056404 (2003).
[22] V. I. Klimov *et al.*, Science **287**, 1011 (2000).
[23] M. Nirmal *et al.*, Nature (London) **383**, 802 (1996).
[24] L. Cognet *et al.*, Proc. Natl. Acad. Sci. U.S.A. **100**, 11 350 (2003).
[25] A. Hartschuh *et al.*, Phys. Rev. Lett. **90**, 095503 (2003).